



The clinical utility of cfRNA for disease detection and surveillance: A proof of concept study in non-small cell lung cancer

Martin Metzenmacher^{1,2}  | Balazs Hegedüs³  | Jan Forster^{4,5} | Alexander Schramm⁶ | Peter A. Horn⁷ | Christoph A. Klein^{8,9} | Nicola Bielefeld^{4,10,11} | Till Ploenes³ | Clemens Aigner³ | Jens T. Siveke^{4,10,11} | Martin Schuler^{1,2,4} | Smiths S. Lueong^{4,10,11}

¹Department of Medical Oncology, West German Cancer Center, University Hospital Essen, Essen, Germany

²Division of Thoracic Oncology, West German Cancer Center, University Medicine Essen Ruhrländlinik, University Duisburg-Essen, Essen, Germany

³Department of Thoracic Surgery, West German Cancer Center, University Medicine Essen Ruhrländlinik, University Duisburg-Essen, Essen, Germany

⁴German Cancer Consortium (DKTK), Partner site University Hospital Essen, Essen, Germany

⁵Chair for Genome Informatics, Department of Human Genetics, University Hospital Essen, University Duisburg-Essen, Essen, Germany

⁶Laboratory for Molecular Oncology, Department of Medical Oncology, West German Cancer Center, University Hospital Essen, University of Duisburg-Essen, Essen, Germany

⁷Institute for Transfusion Medicine, University Hospital Essen, Essen, Germany

⁸Experimental Medicine and Therapy Research, University of Regensburg, Regensburg, Germany

⁹Fraunhofer-Institute for Toxicology and Experimental Medicine, Division of Personalized Tumor Therapy, Regensburg, Germany

¹⁰Bridge Institute of Experimental Tumor Therapy, West German Cancer Center and Division of Solid Tumor Translational Oncology, German Cancer Consortium (DKTK), University Hospital Essen, University Duisburg-Essen, Essen, Germany

¹¹Division of Solid Tumor Translational Oncology, German Cancer Consortium (DKTK, partner site Essen) and German Cancer Research Center, DKFZ, Heidelberg, Germany

Correspondence

Smiths S. Lueong, Bridge Institute for Experimental Cancer Therapy, West German Cancer Center, University Hospital Essen, Hufelandstr. 55, 45147 Essen, Germany.
Email: smiths-sengkwawoh.lueong@uk-essen.de

Funding information

Deutsche Forschungsgemeinschaft (DFG, German Research Foundation), Grant/Award Numbers: SI 1549/3-1, RO 3577/7-1 (KFO 337); European Transcan-2 project CEVIR

Abstract

Background: CT scans are used in routine clinical practice for the diagnosis and treatment surveillance of non-small cell lung cancer (NSCLC). However, more sensitive methods are desirable. Liquid biopsy analyses of RNA and DNA can offer more sensitive diagnostic approaches. Cell-free RNA (cfRNA) has been described in several malignancies, but its clinical utility has not previously been explored.

Methods: We evaluated the clinical utility of cfRNA for early detection and surveillance of tumor disease in a proof-of-concept study. Using real-time-droplet digital polymerase chain reaction we characterized a candidate transcript (*MORF4L2*) in plasma samples from 41 advanced stage, 38 early stage NSCLC and 39 healthy samples. We compared its diagnostic performance with tumor markers and evaluated its utility for disease monitoring.

Results: *MORF4L2* cfRNA was more abundant in patients than in healthy donors ($p < 0.0001$). Using the Youden index approach (cutoff value of 537 copies/ml was established) with a sensitivity of 0.73 (95% CI: 0.61–0.82) and a specificity of 0.87 (95% CI: 0.73–0.96). Positive and negative predictive values of 0.92 (95% CI: 0.83–0.95) and 0.59 (95% CI: 0.47–0.83) were achieved. Combination of cfRNA and Cyfra21-1 improved its predictive value from 89.5% to 94.7%. Low baseline *MORF4L2* levels were associated with better overall survival (HR:0.25, 95% CI: 0.09–0.7, $p = 0.009$) and progression-free survival for patients treated with tyrosine kinase inhibitors ($p = 0.011$) and chemotherapy ($p = 0.019$). *MORF4L2* profile between baseline and follow-up mirrored radiological response and tumor dynamics better than

tumor markers. cfRNA transcripts allowed monitoring tumor dynamics in patients without tumor-reported genetic alterations.

Conclusion: Our data support clinical utility of cfRNA for detection and surveillance of NSCLC. Further studies with larger cohorts are required.

KEYWORDS

cfRNA, ddPCR, liquid biopsy, NGS, NSCLC

INTRODUCTION

Lung cancer, predominantly non-small cell lung cancer (NSCLC), is a major cause of cancer-related deaths worldwide, contributing about 14% of all newly diagnosed cancers.^{1,2} During the past decade, therapeutic advances have improved patient survival. However, the 5-year survival rate is still unacceptably poor. Late stage at diagnosis, given the very few, mostly not specific early symptoms, is a main reason for the observed poor prognosis of long-term survival.^{3,4}

Curative surgery, a therapeutic option offered to early stage cases, improves the 5-year survival rates to 70%–90%.^{5,6} Early and locally advanced stage cases may also receive multimodal treatment modalities comprising systemic treatment, radiotherapy and surgery.^{7–9} Metastatic cases are often not eligible for therapy in curative intent and therefore receive mostly palliative systemic therapies.^{7–9} For these patients, platinum-based chemotherapy with PD-(L)1 checkpoint-inhibition is the appropriate standard of care for the majority of cases.^{7–9} Molecular targeted therapy with tyrosine kinase inhibitors prolongs progression-free survival and is offered to patients with actionable genetic alteration in the *EGFR*-, *BRAF*-, *ALK*- and *ROS1*-genes.^{8,9} Although the different treatment modalities significantly improved patient outcome, resistance-mediated disease progression is almost inevitable. Tools for early detection of biological disease progression and monitoring of treatment response would be of high clinical value. In routine clinical practice, robust and reliable predictive and prognostic markers are rarely available. Treatment monitoring currently mostly relies on radiological imaging. Exposure to ionizing radiation and side effects due to contrast medium can limit the use of these techniques. In effect, radiological imaging can only detect visible increases in tumor mass so that biological disease progression and early onset of treatment failure will be diagnosed only after successful adaptation and growth of the tumor in the course of the current treatment. However, to prevent exposure to ineffective and potentially toxic therapies, disease progression needs to be detected in a timely manner.⁹ Molecular tools, which allow early detection of treatment response and biological disease progression, while providing prognostic insights are highly needed.

Circulating tumor-derived analytes such as circulating tumor DNA and RNA (ctDNA/cfRNA) analysis can enable for repeated observation of disease dynamics^{10,11} and we recently reported the utility of cell-free RNA (cfRNA) for the detection of tumor diseases.¹² cfRNA has previously been reported in malignant melanoma,¹³ nasopharyngeal carcinoma,¹⁴ breast cancer,¹⁵ colorectal cancer,^{16–18} follicular lymphoma¹⁹ and

hepatocellular carcinoma.²⁰ cfRNA has also been reported to allow for determination of gestational age, outperforming conventional markers.²¹ The predictive and prognostic value of cfRNA has until date remained elusive. To address this question in a follow-up of our previous study, we have analyzed close to 120 cfRNA samples from early and late stage NSCLC and healthy controls to evaluate the predictive and prognostic value of selected cfRNA transcripts in NSCLC.

METHODS

Patient cohorts

Patients included in this study were histologically-confirmed lung cancer patients who were prospectively recruited at the outpatient unit of the Department of Medical Oncology at the West German Cancer Center, University Hospital Essen, Essen Germany (stage IV) or at the Department of Thoracic Surgery at the Ruhrlandklinik, West German Cancer Center, University Medicine Essen, Essen Germany (stage I–III). Healthy blood samples were randomly recruited from transfusion blood donors at the Department of Transfusion Medicines at the University Hospital in Essen, Essen Germany. Age of the blood donors was between 18 and 60 years. The local institutional review boards approved the study (17-7740-BO, 14-6056-BO, 14-5961-BO and 17-7729-BO). All participants provided written informed consent.

Blood sampling and radiological assessments

A volume of 7.5 ml of blood was drawn in 7.5 ml EDTA blood tubes (ref no. 01.1605.001, Sarstedt) between 0–2 weeks before the start of systemic treatment or before surgery. Serial blood collection and CT-based response evaluation was organized every eight weeks following two treatment cycles for patients receiving systemic therapy. Plasma was prepared by a three-step centrifugation at 4°C and tumor response was evaluated by CT-scans according to RECIST 1.1. The duration between tumor sampling and blood sampling was less than 10 days.

Plasma cfRNA isolation

Cell-free RNA was isolated using the plasma/serum RNA purification mini kit (cat. 55 000, Norgen Biotek) following the manufacturer's instructions with slight modifications.

Briefly, on column residual DNA digestion was performed on all isolated cfDNA samples as recommended by the manufacturer. Similarly, the lysis buffer was supplemented with β -mercaptoethanol and binding time was increased to 10 min; meanwhile an elution incubation time of 10 was equally used. Sample concentrations were measured with a fluorimeter and samples were stored at -80°C until analyzed. cfRNA was characterized by using the high sensitivity RNA screen tape kit for tape Station (Agilent, cat no. 5067–5579).

Transcript quantification by RT-ddPCR

We previously reported on the utility of cfRNA for disease detection in solid tumors.¹² Based on our data (cfRNA-seq) and analysis of publicly available the cancer genome atlas and gene expression omnibus (GEO) data sets from NSCLC tumors tissues, we identified the most relevant of the differentially abundant protein-coding transcripts for further validation. To this end, all differentially abundant cfRNA transcripts (in both plasma and tumor tissues) were first subjected to feature selection using the Boruta package in R. The most important transcripts were then classified according to their expression levels in NSCLC tumor tissue. We selected the most abundant protein-coding cfRNA transcript, *MORF4L2* for further investigation. Circulating levels of *MORF4L2* transcripts were measured by means of RT-ddPCR using the 1-Step RT-ddPCR Advanced Kit for Probes (Bio-Rad). All reactions were performed in 20 μl duplicate reaction using 2 μl of cfRNA from each sample. The QX100 ddPCR system was used for ddPCR experiments. The average raw *MORF4L2* cfRNA transcript concentration (copies/20 μl reaction) obtained from duplicate reactions, was used to determine the absolute transcript concentration expressed in copies per ml of plasma.

Immunohistochemistry

Immunostaining was performed on 5 μM sections of FFPE tissues using the Dako horse reddish peroxidase one-step polymer (ref no. ZUC053-100, Zytocem Plus). Sections were dewaxed and epitope retrieval was performed in low pH citrate buffer. After blocking, slides were incubated with primary antibodies at 4°C overnight. The slides were then washed and incubated with secondary antibody, then developed using the DAB + chromogen system (Dako). Slides were counterstained with hematoxylin, dehydrated and mounted. Slides were scanned and digitalized with a Zeiss Axio Scanner Z.1 (Carl Zeiss AG).

Statistical analysis

A Mann–Whitney test was used to compare the mean of two groups. Statistical significance was set to a *p*-value

<0.05 . The diagnostic performance of the marker was evaluated with the ROCR package.²² The cutoff threshold between healthy donors and cancer patients for the *MORF4L2* cfRNA transcript was determined using the Youden index as implemented in the R package *OptimalCutPoints* and based on the *MORF4L2* transcript abundance in healthy blood donors. The threshold values were <2.1 ng/mL for CYFRA21-1 and for CEA <2.6 ng/mL according to the used standardized tests from Roche-Cobas and Siemens respectively. The Kaplan–Meier method was used to compare survival differences between groups of patients. Data analysis was performed in the R version 3.6-environment and Graphpad Prism version 7.0 (GraphPad Software, Inc.). Multi- and univariate survival analyses were done using the survival and survminer packages.

RESULTS

Samples and analysis

Plasma samples analyzed in this study were collect either from late stage NSCLC patients (stage IV), early stage NSCLC (stage I–III) or healthy transfusion blood donors (control). Samples from the stage IV patients were collected before initiation of systemic treatment (baseline, T0) and subsequently during each assessment of response to therapy. Samples from the stage I–III patients were collected before surgical resection; meanwhile healthy blood samples were collected from transfusion blood donors. The control cohort consisted of 39 healthy transfusion blood donors, meanwhile the stage I–III cohort was composed of 38 preoperative plasma samples. In the stage IV cohort, 41 pretreatment samples were analyzed, while 28 serial samples from 13 patients were monitored during treatment. Tumor surface area measurements were performed on CT-imaging data. The patient characteristics are reported in Table 1.

Feature selection and characterization

We first identified the most relevant differentially abundant cfRNA transcript from our previous data. There were eight protein-coding cfRNA transcript differentially abundant in patient plasma and tumor tissue. The expression of all protein-coding cfRNA transcripts was assessed in tumor tissue (Figure 1a) and in plasma samples from stage IV patients (Figure 1b). We then used the Boruta feature selection algorithm to identify the most important cfRNA transcript. Of the eight transcripts, five (*C12orf54*, *GLRA3*, *MTFR1*, *TAF1A* and *MORF4L2*) were selected as the most important transcripts (Figure 1c). The expression of all eight transcripts in tumor tissue was then assessed. Of all these transcripts, *MORF4L2* transcript showed the highest expression, with all samples showing more than \log_2 cpm of >10 (Figure 1d). We reasoned that high tumor expression might offer the chance of detecting disease-relevant transcripts in

TABLE 1 Baseline characteristics of patients

	Metastatic/advanced Stage NSCLC (n = 41)	Local Stage NSCLC (n = 38)
Age mean (range)	67 (40–85)	67 (50–88)
Sex:		
Female (%)	22 (53.7)	18 (47.4)
Male (%)	19 (46.3)	20 (52.6)
ECOG		
0 (%)	22 (53.7)	38 (100.0)
1 (%)	16 (39.0)	0 (0.0)
Unknown	3 (7.3)	0 (0.0)
Smoking status		
Active smoker (%)	5 (12.2)	13 (34.2)
Former smoker (%)	26 (63.4)	19 (50.0)
Never smoker (%)	9 (22.0)	5 (13.2)
Unknown (%)	1 (2.4)	1 (2.6)
Stage (IASLC eighth edition)		
IA1–B (%)	0 (0)	20 (52.6)
IIa–b (%)	0 (0)	12 (31.6)
IIIa–c (%)	0 (0)	6 (15.8)
Iva–b (%)	41 (100)	0 (0.0)
Histology		
Adenocarcinoma (%)	30 (73.2)	19 (50.0)
Squamous cell carcinoma (%)	5 (12.2)	14 (36.8)
Adenosquamous carcinoma (%)	3 (7.4)	0 (0.0)
Large cell carcinoma Neuroendocrine (%)	0 (0)	1 (2.6)
Large cell carcinoma (%)	1 (2.4)	4 (10.5)
Not otherwise specified (%)	2 (4.8)	0 (0.0)
Mutational status *		
EGFR-mutated total (%)	7 (17.0)	ND
EGFR exon 19-deletion	6 (12.2)	
EGFR exon 21 L858R- mutation (%)	2 (4.8)	
ALK-translocation (%)	2 (4.8)	
ROS1-translocation (%)	1 (2.4)	
BRAF V600E-mutation (%)	1 (2.4)	
KRAS (total)	7 (17.1)	
KRAS G12C	4 (9.8)	
TP53	12 (29.3)	
RET-translocation (%)	1 (2.4)	
PIK3CA	1 (2.4)	
PD-L1 high expression ** (>50% TPS) (%)	9 (22.0)	

Note: *Tumors can harbor more than one mutation and can additionally show a PD-L1 expression. **Tumors can harbor a mutation beside the high PD-L1 expression. Abbreviations: ECOG, Eastern Cooperative Oncology Group performance index; ND, Not done. At the time of patient recruitment, international guidelines did not recommend that a molecular analyses in patients with localized stage NSCLC, treated with surgery in curative intent should be performed. NSCLC, non-small cell lung cancer. PD-L1, programmed death ligand 1. TPS, tumor proportion score. Percent of viable tumor cells with a positive PD-L1 membrane staining in immunohistochemistry.

circulation and, for this reason, we further analyzed the *MORF4L2* gene. Using RT-ddPCR, we measured the plasma abundance of the *MORF4L2* transcript in plasma from the patient and control cohorts. As shown in Figure 1e, *MORF4L2* cfRNA transcript was significantly abundant in all patients, irrespective of disease stage than in controls. In

tumor tissue, similar patterns were observed for two independent cohorts (TCGA and GSE 81089, Supplementary Figure 1a & 1b). We then wondered if the abundance of *MORF4L2* transcript in circulation was associated with smoking or age. We then categorized our stage IV cohort into never smokers (0 packs/year), light smokers

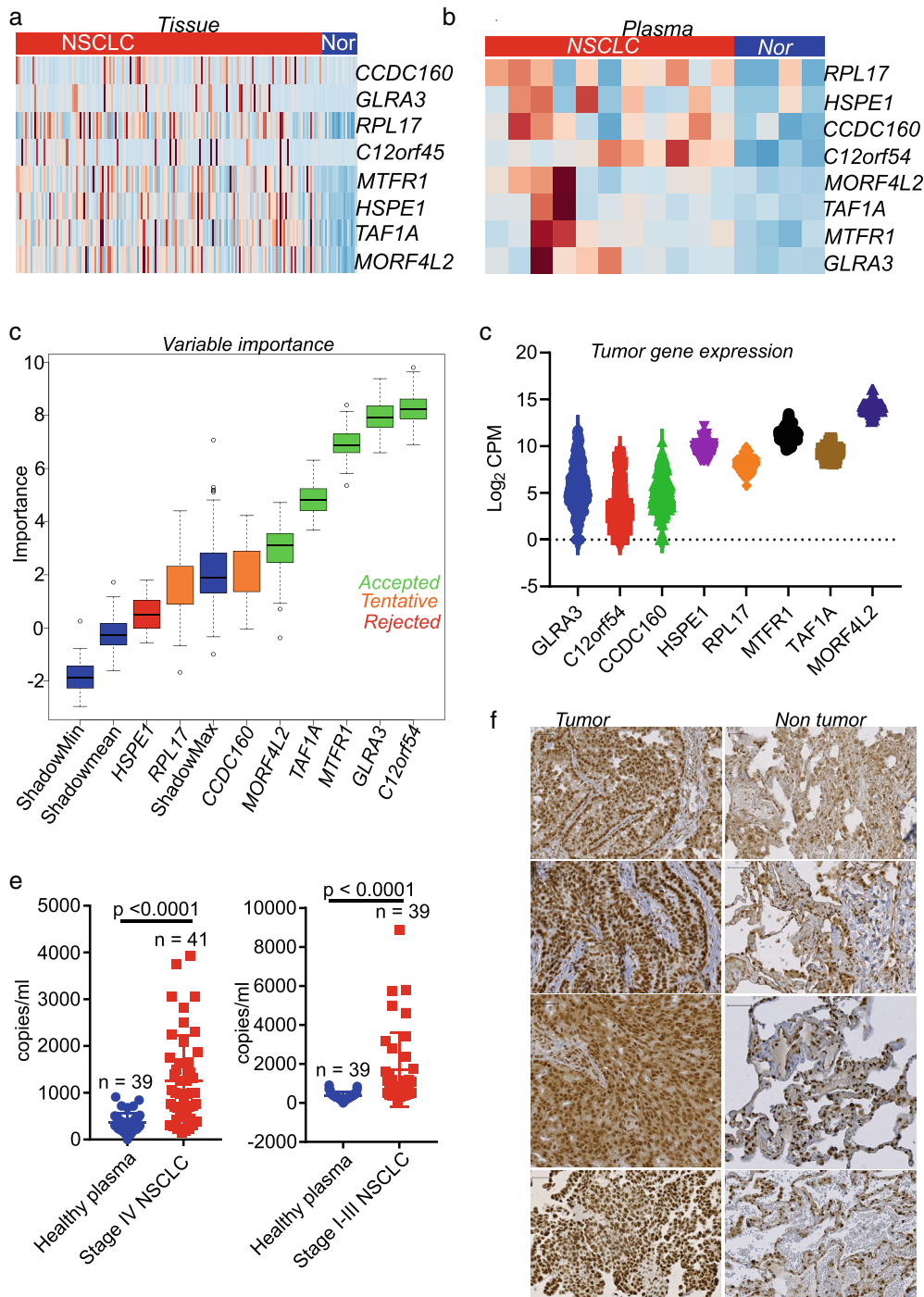


FIGURE 1 Feature selection of candidate protein-coding cRNA transcript. (a) A heatmap showing the expression of all eight protein-coding transcripts that are significantly abundant in patients than controls in NSCLC tumor tissue. These transcripts are an intersection of differentially regulated genes in tumor tissue and patient plasma samples compared with controls. (b) A heatmap showing the expression of all eight patient plasma-derived RNA. The same transcripts as in Figure 1a. (c) A boxplot showing the importance of each of these transcripts in distinguishing patient samples from healthy samples. This boxplot is derived from feature selection using the Boruta R package. (d) A violin plot showing the expression of all eight protein-coding genes in tumor tissue. Data are presented as log₂ cpmand is derived for publicly available RNA-seq from NSCLC patients (GSE81089). (e) The plasma abundance of *MORF4L2* cRNA transcript in stage IV and stage I-III NSCLC patients and healthy controls. The transcript abundance is expressed in copies/ml of plasma used for cRNA isolation. (f) Immunohistochemistry staining of *MORF4L2* protein in tumor tissue samples and adjacent nontumor tissue

(<30 packs/year) and heavy smokers (>30 packs/year). As shown in Supplementary Figure 1c, there was a higher but not significant difference in *MORF4L2* load in the different smoker groups, which was probably due to the low numbers. No obvious difference was observed for different age groups (Supplementary Figure 1c). Comparing *MORF4L2* cRNA abundance in the stage IV and stage I-III group, no obvious significant difference was observed (Supplementary Figure 1e). To establish the tumor relevance of this gene, we performed immunohistochemistry staining on NSCLC and nontumor section and observed a higher number of cells

stained in tumor samples compared to normal tissue (Figure 1f).

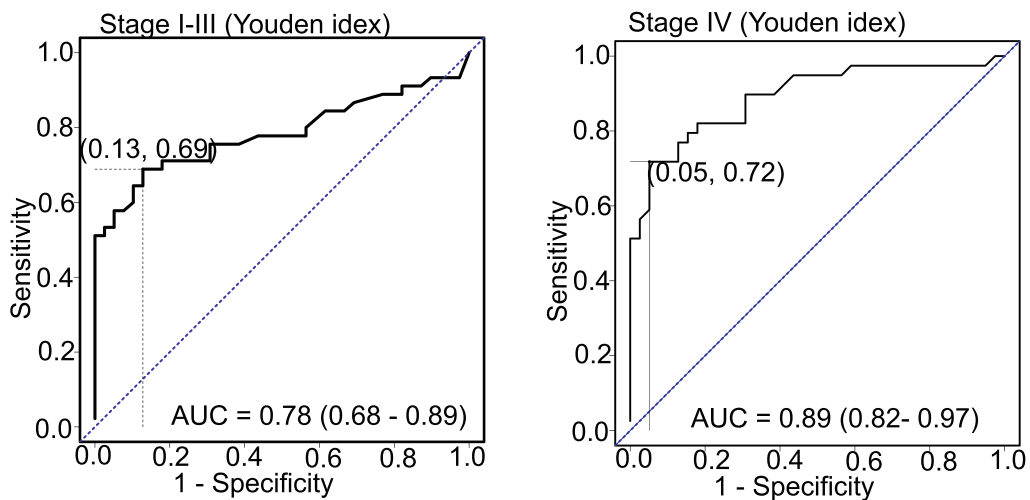
Determination of diagnostic cutoff

Following the identification of the *MORF4L2* cRNA transcript, further proof of concept validation of the clinical utility of cRNA was done. Therefore two algorithms, the Youden index and SpEqualSE as implemented in the R package “OptimalCutpoints”, were used to determine the

a

	Youden index	Stage I-III		SpEqualSe	
Parameter	Estimate	95% CI (lower-upper)		Estimate	95% CI (lower-upper)
cutoff	550 (copies/ml)	-		456.25 (copies/ml)	-
Sensitivity	0.69	0.53 - 0.82		0.71	0.56 - 0.84
Specificity	0.87	0.73 - 0.96		0.72	0.56 - 0.85
Positive predictive value	0.86	0.71 - 0.92		0.74	0.58 - 0.86
Negative predictive value	0.701	0.56 - 0.89		0.68	0.52 - 0.83
		Stage IV			
cutoff	750 (copies/ml)	-		493.75 (copies/ml)	-
Sensitivity	0.72	0.55 - 0.85		0.82	0.66 - 0.92
Specificity	0.95	0.83 - 0.99		0.82	0.66 - 0.92
Positive predictive value	0.93	0.78 - 0.97		0.82	0.66 - 0.92
Negative predictive value	0.77	0.62 - 0.97		0.82	0.66 - 0.92
		All samples			
cutoff	537.5 (copies/ml)	-		468.75 (copies/ml)	-
Sensitivity	0.73	0.61 - 0.82		0.76	0.66 - 0.85
Specificity	0.87	0.73 - 0.96		0.77	0.61 - 0.89
Positive predictive value	0.92	0.83 - 0.95		0.88	0.77 - 0.93
Negative predictive value	0.59	0.47 - 0.83		0.60	0.47 - 0.78

b



c

	cfRNA positive	cfRNA negative	Total
CEA positive	23 (60.5%)	7 (18.4%)	30 (78.9%)
CEA negative	3 (7.9%)	5 (13.2%)	8 (21.1%)
Total	26 (68.5%)	12 (31.5%)	38 (100%)
	cfRNA positive	cfRNA negative	
Cyfra21-1 positive	24 (63.2%)	10 (26.2%)	34 (89.5%)
Cyfra21-1 negative	2 (5.3%)	2 (5.3%)	4 (10.5%)
Total	26 (68.5%)	12 (31.5%)	38 (100%)
	Cyfra-MORF4L2 positive	Cyfra-MORF4L2 Negative	
CEA-MORF4L2 Positive	28 (73.6%)	2 (5.3%)	30 (78.9%)
CEA-MORF4L2 Negative	8 (21.1%)	0 (0%)	8 (21.1%)
Total	36 (94.7%)	2 (5.3%)	38 (100%)

FIGURE 2 The *MORF4L2* cfRNA transcript has diagnostic value. (a) Table showing the diagnostic parameters of the cfRNA transcript in NSCLC patients. The Youden index and SpEqualSe algorithm as implemented in the R package OptimalCutPoints were used. Patients were analyzed independently (stage I-III, $n = 38$ and stage IV, $n = 41$) and as a pool of all patients against a control cohort of $n = 39$. (b) Receiver-operator characteristic curve for stage I-III (left panel) and stage IV (right panel) based on diagnostic values obtained from the Youden index. (c) Cross tabulation comparison of the diagnostic efficacy of *MORF4L2* cfRNA transcript with the tumor markers CEA and Cyfra21-1. Markers were analyzed independently and in combination

diagnostic cutoff values, the sensitivity, specificity as well as the positive and negative predictive values in early and advanced stage NSCLC patients. The diagnostic efficacy of the *MORF4L2* cfRNA transcript was analyzed independently and in combination with the established tumor markers CEA and Cyfra21-1. Although the diagnostic cut-off determined by the Youden index was higher than the value reported by the SpEqualSe algorithm, the diagnostic parameters were closely similar (Figure 2a). We then determined the receiver operator characteristics (ROC) and the area under the ROC curve (AUC). In advanced stage NSCLC patients, the AUC of 0.89, 95%CI (0.82–0.97) was achieved, while an AUC of 0.78, 95% CI (0.68–0.89) was achieved for

the early stage (stage I–III) cases (Figure 2b). Using tumor marker data (CEA and Cyfra21-1), available for 38 stage IV patients, a cross tabulation was made to compare the diagnostic efficacy of cfRNA with established tumor markers. As shown in Figure 2c, 60.5% and 63.2% of patients had values above the cut-off for the combination CEA/*MORF4L2* cfRNA and Cyfra21-1/*MORF4L2* cfRNA, respectively. An additional 7.9% of patients had positive cfRNA values but negative CEA values. Furthermore, 18.4% of patients with negative cfRNA values were positive for CEA, and both markers classified 31.5% of patients as negative. With regards to Cyfra21-1, 26.2% of patients with negative cfRNA values were positive for Cyfra21-1, while 5.3% of Cyfra21-1

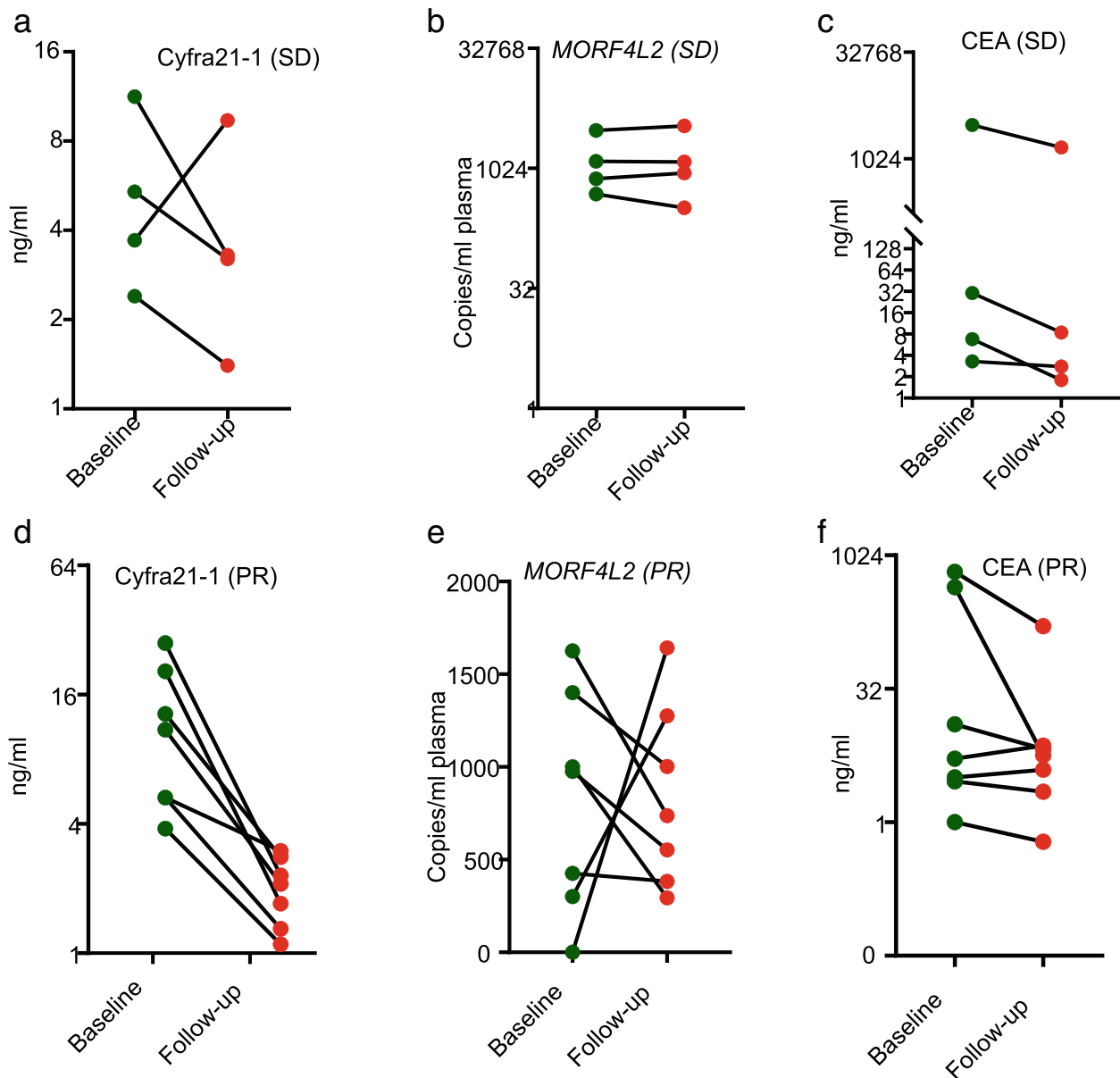


FIGURE 3 Comparative analysis of *MORF4L2* cfRNA transcript and tumor markers for response patterns. (a–c) A line plot showing the profile of the tumor marker Cyfra21-1, the profile of *MORF4L2* cfRNA transcript and the profile of the tumor marker CEA, respectively in patients with radiological stable disease. (d–f) A line plot showing the profile of the tumor marker Cyfra21-1, the profile of *MORF4L2* cfRNA transcript and the profile of the tumor marker CEA, respectively in patients with radiological partial response

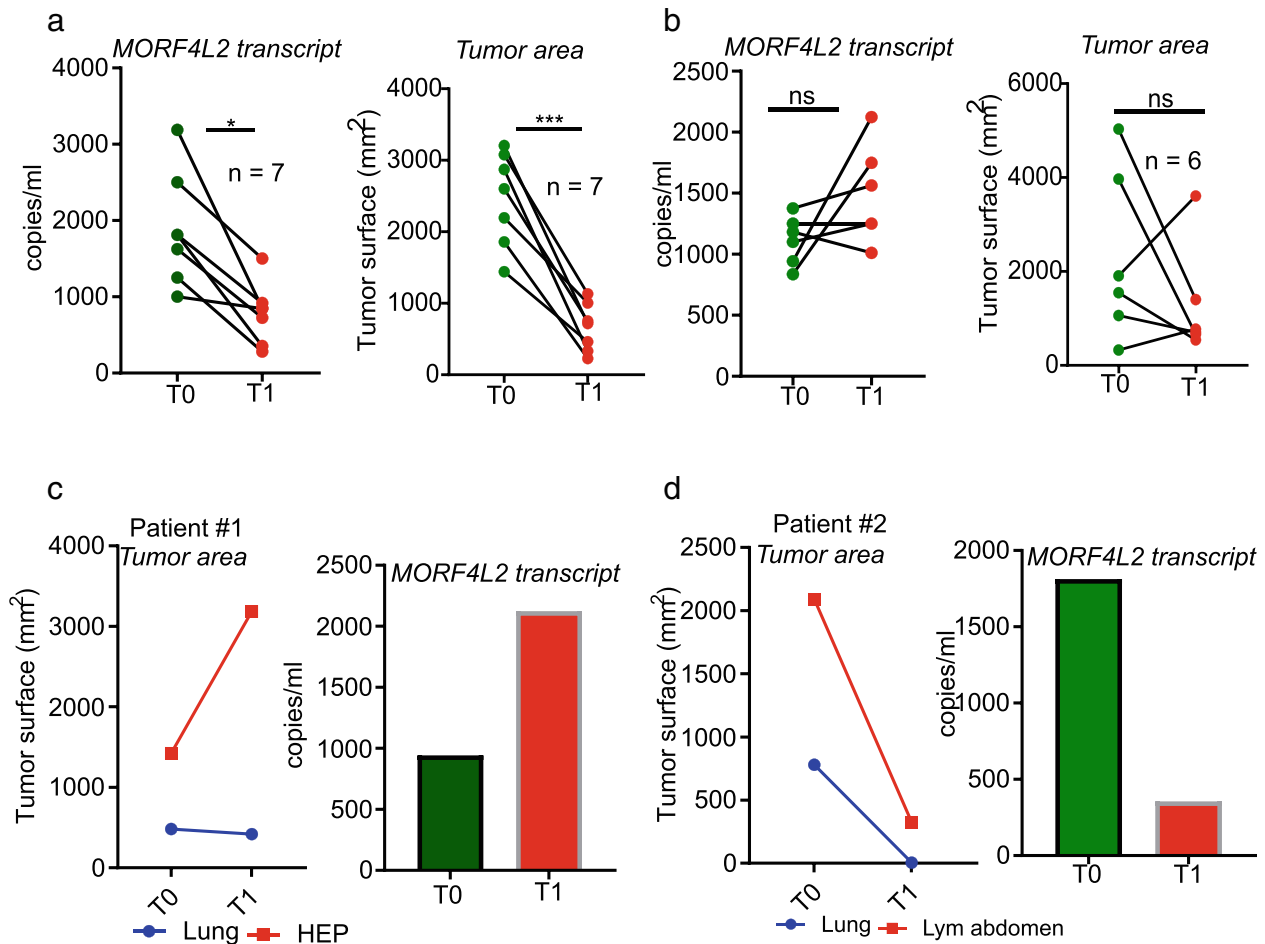


FIGURE 4 Comparative analysis of *MORF4L2* cfrNA transcript profiles and tumor surface area. A line plot showing the *MORF4L2* cfrNA transcript profile and the corresponding tumor surface area measurement between the baseline and first reassessment time point for patients with a significant decrease between both time points (a) and for patients with a stable or increased *MORF4L2* cfrNA transcript profile between both time points (b). (c) A line and bar plot showing the tumor dynamics and *MORF4L2* cfrNA transcript profile, respectively, for a nonresponding patient with two lesions (c) and for a responding patient with two lesions (d)

negative patients had positive cfrNA values. Both markers showed negative values for 5.3% of patients. We then checked if a combination of cfrNA with either of the tumor markers would improve classification. We observed that a combination of cfrNA with Cyfra21-1 increased the percentage of positive patients from 89.5% in Cyfra21-1 alone to 94.7% in the combination. On the other hand, combining CEA and cfrNA did not improve the diagnostic accuracy of CEA, which remained at 78.9%. Taken together, these observations suggest, that cfrNA combination with Cyfra21-1 can increase the diagnostic performance.

Comparative performance of cfrNA and tumor markers for treatment surveillance

We next evaluated the performance of our candidate cfrNA transcript for treatment surveillance as compared with the established tumor markers and by using CT-reported response evaluated by the RECIST criteria. The Cyfra21-1

levels of patients with stable disease (SD) were unstable between baseline and follow-up (first reassessment), with three-quarters of cases decreasing and one quarter of cases increasing (Figure 3a). However, the *MORF4L2* cfrNA profiles for these patients remained stable between both time points and for all patients (Figure 3b). CEA levels for patients with SD were relatively stable compared with the corresponding Cyfra21-1 profiles (Figure 3c). For patients with a partial remission to treatment, Cyfra21-1 levels decreased in all patients and most patients showed tumor marker values below the threshold value (Figure 3d). In the same patients, *MORF4L2* cfrNA levels decreased in most patients, but not below the threshold value, while two patients showed increasing profiles (Figure 3e). These two patients subsequently progressed shortly after the analyzed time point. CEA levels for patients with partial remission were in most cases, stable between the baseline and follow-up time points (Figure 3f). Taken together, these observations suggest, that the *MORF4L2* cfrNA profile reflects the tumor dynamics as reported by RECIST in a comparable

and in some case better manner as established tumor markers.

MORF4L4 cRNA profile reflects CT- tumor dynamics

Following the observation that the *MORF4L2* cRNA transcript can recapitulate tumor marker profiles, we compared CT-reported tumor dynamics during treatment with *MORF4L2* transcript profiles. To this end, we measured the surface area of the tumor at baseline (T0) and at first reassessment with radiological imaging (T1). From the same patients, we quantified the *MORF4L2* cRNA transcript and categorized patients into two groups. On the one hand, were patients with a significant drop in *MORF4L2* cRNA meanwhile patients with a stable or increased *MORF4L2* cRNA

profile were in the second group. When the change in percentage of the transcript between both time points was less than 10%, the profile was considered stable. Based on this criteria, we observed, that patients with a decrease in cRNA transcript also showed a decrease of the tumor surface area between both time points (Figure 4a). Patients with a stable or increased *MORF4L2* cRNA transcript profile showed mixed tumor surface area profiles, with most of them remaining stable or increasing (Figure 4b). We then decided to investigate the behavior of the *MORF4L2* cRNA profiles in patients with multiple lesions. Therefore, we analyzed two patients each with two lesions. In patient no. 1, with a lung and liver lesion, the lung lesion surface area remained stable, while the liver lesion increased about two-fold. We equally observed about twofold increase of the *MORF4L2* cRNA profile in this patient (Figure 4c). In patient #2 with a lung and abdominal lesion, both lesions decreased, with the lung

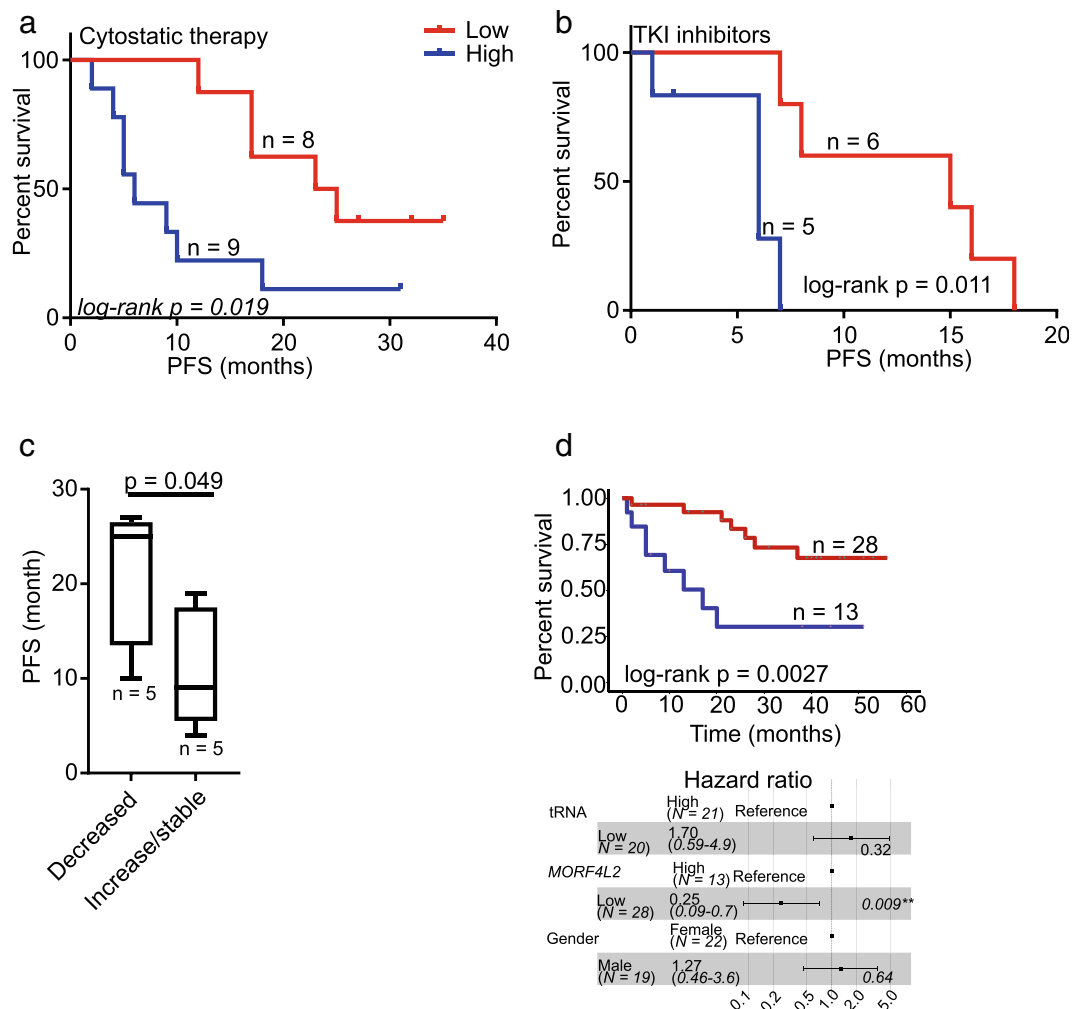


FIGURE 5 Assessment of the prognostic value of *MORF4L2* cRNA. A Kaplan–Meier progression-free survival curve for patients receiving cytostatic therapy either as monotherapy or in combination with immune checkpoint inhibition (a) and for patients receiving tyrosine kinase inhibition as monotherapy (b). A boxplot showing the comparison in the progression-free survival time between patients with a decrease in *MORF4L2* cRNA transcript between baseline and first reassessment and patients with a stable or increased *MORF4L2* cRNA transcript between the baseline and first reassessment time points (c). Kaplan–Meier overall survival curve for all stage IV patients based on the plasma abundance of *MORF4L2* cRNA transcript (upper panel) and a forest plot showing multivariate analysis of the association between *MORF4L2* cRNA transcript and overall survival (lower panel) (d)

lesion decreasing to an undetectable size, while the abdominal lesion decreased almost fourfold. We also observed about 3.5-fold decrease in the *MORF4L2* cfRNA transcript profile for this patient (Figure 4d). These two patients were selected because patient no.1 had a tissue-reported *KRAS* mutation, which could not be detected in plasma, meanwhile patient no. 2 had no tissue-reported actionable mutation. These patients would otherwise not have been eligible for ctDNA-based monitoring approaches in clinical routine.

MORF4L2 cfRNA transcript predicts patient outcome

cfRNA from 41 stage IV NSCLC patients were analyzed by RT-ddPCR. Patients were treated either with tyrosine kinase inhibitors (TKI), immune checkpoint inhibitors (CPI) and cytostatic monotherapy plus CPI. The groups of patients who received TKI or cytostatic therapy were larger than the others and we dichotomized these two groups at the median expression of *MORF4L2* in all samples. High baseline expression of *MORF4L2* was associated with shorter progression-free survival for patients receiving cytostatic therapy + CPI and TKIs (Figure 5a & b respectively). We then checked if decrease in *MORF4L2* cfRNA transcript between T0 and T1 was associated with better progression-free survival (PFS). In effect, patients with decreased transcript levels between both time points demonstrated a longer PFS than patients with a stable or increased transcript pattern (Figure 5c). In the next step the overall survival of all 41 stage IV patients was computed relative to the baseline *MORF4L2* transcript levels. As shown in Figure 5d (upper panel), high plasma levels of *MORF4L2* transcript were associated with poor overall survival. It was also analyzed if other factors, such as gender or the amount of cfRNA, could affect the predictive value of this cfRNA transcript. Low levels of *MORF4L2* cfRNA transcript were associated with better overall survival (OS) (HR: 0.25, 95% CI: 0.09–0.7, p -value = 0.009) (Figure 5d, lower panel). The total amount of cfRNA as well as patients gender showed no significant effect regarding OS.

DISCUSSION

We investigated the clinical utility of cfRNA for early detection and monitoring disease dynamics in non-small cell lung cancer. Patient samples were collected during routine clinical visits to simulate a real-life situation. All blood samples were processed within 2 h of blood draw or stored at 4°C for less than 4 h. Previous studies have shown that unlike serum, plasma storage at 4°C for up to 24 h does not affect cfRNA quality.²³ Total cfRNA yield per ml of plasma varied between 1.7–31 ng. Despite stability challenges, others and us have shown that cfRNA is a potential source of clinically-relevant information in cancer as well as in nonmalignant diseases.^{12,24,25} For this proof-of-concept study, we selected

a previously identified cfRNA transcript, *MORF4L2*, which was found to be strongly abundant in patient plasma compared with healthy transfusion blood donors. The focus on the *MORF4L2* transcript was motivated by its high tumor expression levels and strong association with disease phenotype. Interestingly, this transcript has been reported to be involved in treatment relapse in NSCLC.²⁶

The plasma abundance of this transcript was measured by means of RT-ddPCR in plasma samples from NSCLC patients and healthy transfusion blood donors. We then used the Youden index and the SpEqualSe algorithms to determine a diagnostic cutoff value. The sensitivity as well as specificity were very good (>0.7) and the positive and negative predictive values were good and modest, respectively (>0.9 and 0.5, respectively). Combining *MORF4L2* cfRNA with the tumor marker Cyfra21-1, did improve its diagnostic performance. Higher plasma levels of *MORF4L2* cfRNA transcript, before start of treatment, were associated with poor overall and progression-free survival for patients who received TKIs and cytostatic therapy+/- CPI. In effect, high levels of a tumor-associated transcript in plasma maybe reflective of high cellular turnover and tumor growth.²⁷ Furthermore, *MORF4L2* has been associated with enhanced tumor initiation in vivo, following treatment.²⁶ Higher cfRNA levels of this transcript may indeed be suggesting disease progression or new metastatic manifestations that are below the CT detection limits.

Decrease in *MORF4L2* cfRNA transcript concentration between baseline and first reassessment was associated with decrease in tumor surface area while stable or increased cfRNA profile was associated with a mixture of radiological responses. We further investigated the influence of total cfRNA yield and found no correlation between *MORF4L2* cfRNA transcript abundance and total sample cfRNA yield. These findings are in line with our previous observation, where cfRNA transcripts from epithelial sources distinguishes patients and healthy blood donors and support the tumor cell origin of this transcript. Using cfRNA transcript abundance, we could also monitor the disease profile of patients with no measurable genetic alteration, as well as patients with tumor-reported genetic alterations which however could not be found in the corresponding plasma sample. The cfRNA transcript profile of *MORF4L2* mirrored tumor dynamics, derived from CT-scans, in a comparable or better manner as tumor markers.

It is therefore very likely that cfRNA can be used to complement other approaches to monitor patient's tumor dynamics independent of mutational status and despite tumor heterogeneity. Our study is limited by the lack of mechanistic information relating to the stabilization of cfRNA in blood and the limited number of patients analyzed in this proof-of-concept study. Until such gaps are filled, we believe that timely and proper sample handling can allow for cfRNA preservation. Taken together our data support clinical utility of cfRNA both for disease detection, but most importantly for response prediction and patient prognosis.

In conclusion, here we provided evidence that the cRNA transcript *MORF4L2* is useful for diagnostic and prognostic purposes as well as for monitoring response to therapy. Further investigation with larger sample cohorts are needed to establish the diagnostic strength of such markers and their utility for monitoring in clinical routine as a possible supplement or substitute for radiological monitoring of anticancer therapy.

ACKNOWLEDGMENT

Human biological samples and related data were provided by the Westdeutsche Biobank Essen (WBE, University Hospital Essen, University of Duisburg-Essen, Essen, Germany).

This work was supported by a European Transcan-2 project CEVIR and the German Cancer Consortium (DKTK). SSL was partially supported by the Deutsche Forschungsgemeinschaft (DFG, German Research Foundation)—SI 1549/3-1 and RO 3577/7-1 (KFO 337).

The laboratory of JTS is supported by the German Cancer Consortium (DKTK). Open Access funding enabled and organized by Projekt DEAL.

CONFLICT OF INTEREST

MM reports outside the submitted work honoraria for advisory boards from Astra Zeneca, Amgen, Boehringer Ingelheim BMS, MSD, Novartis, Roche, Takeda.

JTS receives honoraria as consultant or for continuing medical education presentations from AstraZeneca, Bayer, Immunocore, Roche, Servier. His institution receives research funding from Bristol-Myers Squibb, Celgene, Roche; He holds ownership and serves on the Board of Directors of Pharma15, all outside the submitted work.

MS reports outside the submitted work honoraria as consultant for Amgen, AstraZeneca, BIOCAD, Boehringer Ingelheim, Bristol-Myers Squibb, GlaxoSmithKline, Janssen, Merck Serono, Novartis, Roche, Sanofi, Takeda, honoraria for CME presentations from Amgen, Boehringer Ingelheim, Bristol-Myers Squibb, Janssen, Novartis and Research funding to institution from AstraZeneca, Bristol Myers-Squibb.

All other authors report no conflict of interest.

ORCID

Martin Metzenmacher  <https://orcid.org/0000-0001-5395-9010>

Balazs Hegedüs  <https://orcid.org/0000-0002-4341-4153>

REFERENCES

- Sung H, Ferlay J, Siegel RL, Laversanne M, Soerjomataram I, Jemal A, et al. Global cancer statistics 2020: GLOBOCAN estimates of incidence and mortality worldwide for 36 cancers in 185 countries. *CA Cancer J Clin.* 2021;71:209–49.
- Herbst RS, Morgensztern D, Boshoff C. The biology and management of non-small cell lung cancer. *Nature.* 2018;553:446–54.
- Gridelli C, Rossi A, Carbone DP, Guarize J, Karachaliou N, Mok T, et al. Non-small-cell lung cancer. *Nat Rev Dis Primers.* 2015;1:15009.
- Lai Y, Wang X, Zeng T, Xing S, Dai S, Wang J, et al. Serum VEGF levels in the early diagnosis and severity assessment of non-small cell lung cancer. *J Cancer.* 2018;9:1538–47.
- Blandin Knight S, Crosbie PA, Balata H, Chudziak J, Hussell T, Dive C. Progress and prospects of early detection in lung cancer. *Open Biol.* 2017;7:9.
- Goldstraw P, Chansky K, Crowley J, Rami-Porta R, Asamura H, Eberhardt WE, et al. The IASLC lung cancer staging project: proposals for revision of the TNM stage groupings in the forthcoming (eighth) edition of the TNM classification for lung cancer. *J Thorac Oncol.* 2016;11:39–51.
- Hoekstra CJ, Hoekstra OS, Stroobants SG, Vansteenkiste J, Nuyts J, Smit EF, et al. Methods to monitor response to chemotherapy in non-small cell lung cancer with 18F-FDG PET. *J Nucl Med.* 2002;43:1304–9.
- Planchard D, Popat S, Kerr K, Novello S, Smit EF, Faivre-Finn C, et al. Metastatic non-small cell lung cancer: ESMO clinical practice guidelines for diagnosis, treatment and follow-up. *Ann Oncol.* 2018;29:192–237.
- Hanna N, Johnson D, Temin S, Baker S, Brahmer J, Ellis PM, et al. Systemic therapy for stage IV non-small-cell lung cancer: American Society of Clinical Oncology clinical practice guideline update. *J Clin Oncol.* 2017;35:3484–515.
- Wan JCM, Massie C, Garcia-Corbacho J, Mouliere F, Brenton JD, Caldas C, et al. Liquid biopsies come of age: towards implementation of circulating tumour DNA. *Nat Rev Cancer.* 2017;17:223–38.
- Diehl F, Schmidt K, Choti MA, Romans K, Goodman S, Li M, et al. Circulating mutant DNA to assess tumor dynamics. *Nat Med.* 2008;14:985–90.
- Metzenmacher M, Varaljai R, Hegedus B, Cima I, Forster J, Schramm A, et al. Plasma next generation sequencing and droplet digital-qPCR-based quantification of circulating cell-free RNA for noninvasive early detection of cancer. *Cancers (Basel).* 2020;12:2.
- Kopreski MS, Benko FA, Kwak LW, Gocke CD. Detection of tumor messenger RNA in the serum of patients with malignant melanoma. *Clin Cancer Res.* 1999;5:1961–5.
- Lo KW, Lo YMD, Leung SF, Tsang YS, Chan LYS, Johnson PJ, et al. Analysis of cell-free Epstein-Barr virus-associated RNA in the plasma of patients with nasopharyngeal carcinoma. *Clin Chem.* 1999;45:1292–4.
- Chen XQ, Bonnefoi H, Pelte MF, Lyautey J, Lederrey C, Movarekhi S, et al. Telomerase RNA as a detection marker in the serum of breast cancer patients. *Clin Cancer Res.* 2000;6:3823–6.
- Silva JM, Dominguez G, Silva J, Garcia JM, Sanchez A, Rodriguez O, et al. Detection of epithelial messenger RNA in the plasma of breast cancer patients is associated with poor prognosis tumor characteristics. *Clin Cancer Res.* 2001;7:2821–5.
- Chuen S, Wong C, Fong S. Quantification of plasma beta-catenin mRNA in colorectal cancer and adenoma patients (vol 10, pg 1613, 2004). *Clin Cancer Res.* 2006;12:996.
- Wong SCC, Lo SFE, Cheung MT, Ng KOE, Tse CW, Lai BSP, et al. Quantification of plasma beta-catenin mRNA in colorectal cancer and adenoma patients. *Clin Cancer Res.* 2004;10:1613–7.
- Dasi F, Lledo S, Garcia-Granero E, Ripoll R, Marugan M, Tormo M, et al. Real-time quantification in plasma of human telomerase reverse transcriptase (hTERT) mRNA: a simple blood test to monitor disease in cancer patients. *Lab Invest.* 2001;81:767–9.
- Miura N, Shiota G, Nakagawa T, Maeda Y, Sano A, Marumoto A, et al. Sensitive detection of human telomerase reverse transcriptase mRNA in the serum of patients with hepatocellular carcinoma. *Oncol -Basel.* 2003;64:430–4.
- Ngo TTM, Moufarrej MN, Rasmussen MLH, Camunas-Soler J, Pan WY, Okamoto J, et al. Noninvasive blood tests for fetal development predict gestational age and preterm delivery. *Science.* 2018;360:1133–6.
- Sing T, Sander O, Beerenwinkel N, Lengauer T. ROCr: visualizing classifier performance in R. *Bioinformatics.* 2005;21:3940–1.
- Tsui NB, Ng EK, Lo YM. Stability of endogenous and added RNA in blood specimens, serum, and plasma. *Clin Chem.* 2002;48:1647–53.

24. Beck TN, Bumber YA, Aggarwal C, Pei J, Thrash-Bingham C, Fittipaldi P, et al. Circulating tumor cell and cell-free RNA capture and expression analysis identify platelet-associated genes in metastatic lung cancer. *BMC Cancer*. 2019;19:603.
25. Ibarra A, Zhuang J, Zhao Y, Salathia NS, Huang V, Acosta AD, et al. Non-invasive characterization of human bone marrow stimulation and reconstitution by cell-free messenger RNA sequencing. *Nat Commun*. 2020;11:400.
26. Kuo WY, Wu CY, Hwu L, Lee JS, Tsai CH, Lin KP, et al. Enhancement of tumor initiation and expression of KCNMA1, MORF4L2 and ASPM genes in the adenocarcinoma of lung xenograft after vorinostat treatment. *Oncotarget*. 2015;6:8663–75.
27. Labi V, Erlacher M. How cell death shapes cancer. *Cell Death Dis*. 2015;6:e1675.

SUPPORTING INFORMATION

Additional supporting information can be found online in the Supporting Information section at the end of this article.

How to cite this article: Metzenmacher M, Hegedüs B, Forster J, Schramm A, Horn PA, Klein CA, et al. The clinical utility of cfRNA for disease detection and surveillance: A proof of concept study in non-small cell lung cancer. *Thorac Cancer*. 2022;13(15):2180–91. <https://doi.org/10.1111/1759-7714.14540>